CEN/WS 71

Date: June 2014

CEN CWA xxxx

CEN/WS 71

Secretariat: SNV

Validation of computational solid mechanics models

ICS:

Descriptors:

Document type: CWA
Document subtype:
Document stage: Draft for Comment
Document language: English

Contents

Page

Foreword

This CEN Workshop Agreement has been drafted and approved by a Workshop of representatives of interested parties on 2014-06-11, the constitution of which was supported by CEN following the public call for participation made on 2013-02-27.

A wide range of organizations were consulted during the preparation of this agreement and were drawn from the following economic sectors: Aerospace; Automotive; Instrument manufacturing; Nuclear power; Research institutes and Universities. The following individuals have contributed to and support the technical consensus represented by this CEN Workshop Agreement:

Erwin Hack	Eidgenoessische Materialpruefungs-und Forschungsanstalt (EMPA), Switzerland
Alexander Ihle	High Performance Space Structure Systems GmbH, Germany
Hannah Jones	University of Liverpool, England
George Lampeas	University of Patras, Greece
Eann Patterson	University of Liverpool, England
Andrea Pipino	Centro Ricerche FIAT SCPA, Italy
Paul Ramsay	National Nuclear Laboratory Limited, England
Olaf Reichmann	High Performance Space Structure Systems GmbH, Germany
Thorsten Siebert	Dantec Dynamics GmbH, Germany
Nassia Tzelepi	National Nuclear Laboratory Limited, England
Rolf Widmer	Schweizerische Normen-Vereinigung (SNV), Switzerland

These individuals and their employers accept no responsibility for the use of designs and protocols described in this Agreement or for the correctness of the results obtained from them and no legal liability in contract tort or otherwise shall attend to these individuals or their employers arising out of the use of the information contained in this Agreement.

The financial support of EU FP7 project VANESSA (grant no. 319116) in the preparation of this document is acknowledged.

The formal process followed by the Workshop in the development of the CEN Workshop Agreement has been endorsed by the National Members of CEN but neither the National Members of CEN nor the CEN-CENELEC Management Centre can be held accountable for the technical content of the CEN Workshop Agreement or possible conflict with standards or legislation. This CEN Workshop Agreement can in no way be held as being an official standard developed by CEN and its members.

The final review/endorsement round for this CWA was started on 2014-05-10 and was successfully closed on 2014-06-10. The final text of this CWA was submitted to CEN for publication on 2014-06-30.

This CEN Workshop Agreement is publicly available as a reference document from the National Members of CEN: Austria, Belgium, Bulgaria, Croatia, Cyprus, Czech Republic, Denmark, Estonia, Finland, France, Germany, Greece, Hungary, Iceland, Ireland, Italy, Latvia, Lithuania, Luxembourg, Malta, Netherlands, Norway, Poland, Portugal, Romania, Slovakia, Slovenia, Spain, Sweden, Switzerland, Turkey and the United Kingdom. (*to be completed at the day of publication*)

Comments or suggestions from the users of the CEN Workshop Agreement are welcome and should be addressed to the CEN-CENELEC Management Centre.

0. Introduction

0.1. Engineering simulation is an essential feature in the design and manufacture of all engineered products at all scales. In particular, simulation based on computational solid mechanics models permits designers to optimise the load-bearing components in devices, machines and structures so that a satisfactory level of reliability is achieved for an acceptable cost. The desire for a sustainable society stimulates designers to create elegant, light-weight designs in which embodied energy and material is minimised; however at the same time consumers demand "total reliability" that often can be achieved most easily by heavy, conservative designs in which additional material provides additional factors of safety. Removal of these safety factors to create light-weight and efficient designs requires a very high level of confidence in the engineering simulations. This confidence level should be acquired through rigorous, quantitative validation of the models employed for the simulations. Although many engineering companies and organisations have developed internal procedures for validating the computational models that are essential to their engineering design activities, there are no standards for the validation of computational solid mechanics models used in engineering design. Consequently, many engineering artefacts are designed using inadequately validated computational models which when this is recognised leads to conservative design, and when it is not recognised leads to unreliable design. The lack of standardisation inhibits the exchange of both data from simulations and of models used for simulation, which in turn slows down innovation, particularly in industries producing engineering systems that are composed of many sub-systems produced by different manufacturers. This CWA aims to address this short-fall.

0.2. The terms 'model' and 'simulation' are often used interchangeably in the engineering community. In this document the term 'simulation' is taken to mean 'the imitation of behaviour or operation of a real-world system or process' and it is assumed that a computational model is used to perform the simulation. A 'computational solid mechanics model' describes the response of a solid medium subject to loading, more specifically it relates the loading conditions, the material behaviour and the response of an object. The material behaviour is usually introduced in computational solid mechanics models using constitutive equations which can be termed 'constitutive models'.

0.3. Computational solid mechanics models are, in general, based on the finite element method[1] with some use of the boundary element method[2]. A large number of commercially available software packages provide end-users with varying degrees of modelling capability based on these methods. It is the norm for the suppliers of these packages to perform verification of the modelling method; in which verification is defined as *'The process of determining that a computational model accurately represents the underlying mathematical model and its solution'*[3]. However, it is the responsibility of the user to perform adequate validation of each model developed with a package. Validation is defined as *'The process of determining the degree to which a model is an accurate representation of the real world from the perspective of the intended uses of the model'*[4]. A large number of benchmarks are provided by e.g. NAFEMS[5] to support vendors and users in verifying finite element packages; but support for the validation process is almost non-existent. The American Society of Mechanical Engineers has developed a Guide for Verification and Validation of Computational Solid Mechanics[4] which describes what is required but does not provide any methodology for performing a validation. The objective of this CEN Workshop Agreement is to fill this gap by providing a general approach to the validation of computational solid mechanics models used in engineering design and evaluation of structural integrity.

0.4. At the moment there are no directives or relevant national legislation and very little documentation in the form of standards or standardization related activities concerned with the validation of computational solid mechanics models. The United States Department of Defense issued a

[1] Zienkiewicz, O.C., & Taylor, R.L., The finite element method: basic formulation and linear problems, McGraw-Hill, New York, 1989.

[2] Banerjee, P.K., Butterfield, R., Boundary element methods in engineering science, McGraw-Hill Book Co., London, 1981.

[3] Computational Fluid Dynamics Committee on Standards, "Guide for Verification and Validation of Computational Fluid Dynamics Simulations," American Institute of Aeronautics and Astronautics, AIAA G-077-1998, ISBN 1-56347-285-6, January 1998.

[4] ASME V&V 10-2006, Guide for verification & validation in computational solid mechanics, American Society of Mechanical Engineers, New York, 2006.

[5] National Agency for Finite Element Methods and Standards, www.nafems.org

glossary of terminology for modelling and simulation in 1998[6], while the American Society for Testing of Materials has published a "Standard Guide for Evaluating Non-Contacting Optical Strain Measurement Systems"[7], which describes the principal approach for obtaining data for the validation process. There has been some activity in the scientific literature with Schwer[8] describing in outline the 'Guide for verification and validation in computational solid mechanics'[4]. He identified that verification can be achieved largely without reference to the real-world. Whereas, validation should be achieved by reference to experiments conducted specifically for this purpose.

0.5. The traditional approach to validation of computational solid mechanics models is to obtain experimental data from strain gauges bonded to a physical realisation of the model at locations of high stress indicated by the simulation. There are two major flaws with this approach: (i) the locations of highest stress may be elsewhere than predicted by the simulation and could lead to component failure; and (ii) no validation is performed in regions of apparently low stress where the design might be optimised by removal of material mass, so again increased stress in these regions could lead to component failure.

0.6. More comprehensive data-fields from experiments are available for validation via the use of optical techniques such as digital image correlation, photoelasticity, and thermoelastic stress analysis. These techniques provide data over a full field of view, and thus generate maps of displacement, strain or stress containing of the order of 10^6 data points, which is comparable to the number of nodes found in computational models. A point-by-point comparison of such data-rich maps from different sources and in different coordinate systems is computationally expensive, maybe impractical, and leads to a result that is not useful or at least cumbersome to interpret. Consequently, it is common practice to extract sections of experimental data from such maps for comparison to values predicted by simulations [e.g. 9, 10, 11] and, while this is an improvement on validation compared to using data from a small number of points at which strain gauges are located, it falls short of the comprehensive, quantitative validation that is sought to provide high levels of confidence in engineering design simulations.

0.7. The output from the validation process needs to be in a format that allows decision-makers to quantify their confidence in the computational models used in the design process. A key step in this quantification is establishing the uncertainty in the experimental data. The uncertainty in the data maps from experiment can be evaluated via the calibration of the optical system employed for their measurement[12,13,14]. More recently, the reliability of data collected in experiments involving variable amplitude loading has been considered, and statistical methods have been developed to quantify the associated uncertainties based on probability density functions[15]. Calibration provides traceability via a continuous chain of comparisons to an international standard, in this case for length, and also allows the measurement uncertainty to be established. Traceability is important in areas such as aerospace and nuclear power, which require certification of designs by regulatory

---

[6] DoD Modeling and Simulation Glossary, Under Secretary of Defense of Acquisition Technology, Washington DC., January 1998, available at www.dtic.mil/whs/directives/corres/pdf/500059m.pdf

[7] ASTM E2208 - 02(2010)e1 Standard Guide for Evaluating Non-Contacting Optical Strain Measurement Systems, American Society for Testing of Materials, West Conshohocken, PA, 2010.

[8] Schwer, LE., An overview of the PTC 60/V&V 10: guide for verification and validation in computation solid mechanics, *Engineering with Computers*, 23, 245-252, 2007.

[9] De Strycher, M., Lava, P.,van Paepegem, W., Schueremans, L., Debruyne, D., Validation of welding simulations using thermal strains measured using DIC, *Applied Mechanics and Materials*, 70, 129-134, 2011

[10] Lomov, SV., Ivanov, DS., Verpoest, I., Zako, M., Kurashiki, T., Nakai, H., Molimard, J., Vautrain, A., Full-field strain measurements for validation of meso-FE analysis of textile composites, *Composites A: Applied Science and Manufacturing*, 39(8):1218-1231, 2008.

[11] Miao, HY., Larose, S., Perron, C., Lévesque, M., Numerical simulation of the stress peen forming process and experimental validation, *Advances in Engineering Software*, 42(11):963-975, 2011.

[12] Patterson, E.A., Hack, E., Brailly, P., Burguete, R.L., Saleem, Q., Siebert, T., Tomlinson, R.A., & Whelan, M.P., Calibration and evaluation of optical systems for full-field strain measurement, *Optics and Lasers in Engineering*, 45(5):550-564, 2007.

[13] Sebastian, C., Patterson, E.A., Calibration of a digital image correlation system, *Experimental Techniques*, doi. 10.1111/ext.12005, 2014.

[14] Whelan, M.P., Albrecht, D., Hack, E., Patterson, E.A., Calibration of a speckle interferometry full-field strain measurement system, *Strain*, 44(2):180-190, 2008.

[15] Baharin, MN., Nopiah, ZM., Abdullah, S., Khairir, MI., Lennie, A., The development of validation technique in variable amplitude loadings strain repetitive data collection, *Key Engineering Materials*, 462-463:337-342, 2011.

authorities. The establishment of measurement uncertainties is critical in making quantitative judgments about comparisons between datasets.

0.8. Recently, it has been proposed that a comparison of maps of strain and displacement data from computational models and experiments can be performed straightforwardly using shape descriptors[16]. Since these maps contain some level of redundant information, shape descriptors, which are rotation, scale and translation invariant, provide an effective means of comparison. Shape descriptors, including geometric moments, Fourier descriptors and wavelet descriptors are used in the field of image analysis for applications such as finger print recognition[17], face recognition[18], target recognition[19], and medical diagnostics [20]. They allow the decomposition of high resolution images into only a hundred or less unique moments, which are a faithful representation of the relevant features in the corresponding image. Recently[21], it has been demonstrated that a comparison of two sets of shape descriptors[22], describing the strain maps obtained from digital image correlation and computational modelling, can be used to update a finite element model[23] and improve its fidelity. These studies are innovative because they treat maps of strain as images and represent them with a small number of information-preserving moments which allows statistical measures to be applied effectively.

0.9. This CWA builds on the philosophy and recent advances described above to provide a methodology for validating computational solid mechanics models in a manner that is consistent with existing guidelines [4,6,7].

[16] Sebastian, C., Hack, E., Patterson, EA., An approach to the validation of computational solid mechanics models for strain analysis*, J. Strain Analysis*, 48(1):36-47, 2013.

[17] Ismail RA., Ramadan MA., Danf TE., and Samak AH., Multi-resolution Fourier-Wavelet descriptors for fingerprint recognition. *Int. Conf. on Computer Science and Information Technology,* 951- 955, 2008.

[18] Nabatchian A., Abdel-Raheem E., and Ahmadi M., 2008, Human face recognition using different moment invariants: a comparative review. *Congress on Image and Signal Processing*, 661-666, 2008.

[19] Bhanu B., and Jones T.L., Image understanding research for automatic target recognition. *IEEE Aerospace and Electronic Systems Magazine*, 15-22, 1993.

[20] Ahmad, WSHMW, & Fauzi, MFA., Comparison of different feature extraction techniques in content based image retrieval for CT brain images. *IEEE 10th workshop on multimedia signal processing, Cairns,* 503-508, 2008.

[21] Wang, W., Mottershead, JE., Sebastian, CM., Patterson, EA., Shape features and finite element model updating from full-field strain data, *Int. J. Solids Struct*. 48(11-12), 1644-1657, 2011

[22] Teague, MR, Image analysis via the general theory of moments. *J. Opt. Soc. America*, **70**, 920-930, 1980.

[23] Friswell, MI., Mottershead, JE., *Finite Element Model Updating in Structural Dynamics*, Kluwer Academic Publishers, 1995.

1. Scope

1.1. This CEN Workshop Agreement (CWA) builds on the research outputs of two completed projects from the European Commission's Framework Programmes FP5 and FP7 with the aim of supporting their implementation in engineering industry and the related research community. The FP5 project SPOTS (Standardisation Project for Optical Techniques of Strain measurement) led to a unified calibration methodology for all optical systems capable of measuring strain fields on planar surfaces of engineering components subject to static and pseudo-static loading[12-14]. The SPOTS project provided an initial step in the process of validating computational solid mechanics models by creating a route for providing high quality data from experiments which is a pre-requisite in the validation process.

1.2. The FP7 project ADVISE[24] extended the research outputs from SPOTS in two important areas, i.e. developing an efficient quantitative method of comparing very large datasets[16,21] based on image decomposition and extending the calibration methodology to include dynamic and out-of-plane loading of engineering components.

1.3. This CWA includes both a protocol for validation of computational solid mechanics models using data-fields from calibrated instruments and a methodology for the calibration of optical systems for measurement of displacement and strain fields in static and dynamic loading. These procedures provide a general approach to the validation of computational solid mechanics models used in engineering design and the evaluation of structural integrity.

1.4. This CWA exploits a number of very powerful optical measurement techniques for acquiring displacement and strain data in engineering components subject to service loads[25], of which digital image correlation is becoming ubiquitous. These techniques generate high-density maps of displacement and strain containing of the order of 10^5 to 10^6 data values per view, which with careful experimental design could cover the majority of the surface of an engineering component. This CWA provides a procedure for the quantitative comparison of such data with corresponding data generated by engineering simulations based on computational solid mechanics models.

1.5. This CWA proposes the use of image decomposition to allow displacement and strain fields to be represented by feature vectors, which are invariant to rotation, scale and translation, and allow enormous data compression while preserving all of the relevant information[21]. A validation protocol is described, based on this data compression, that is efficient to apply, takes into account uncertainties, and gives a quantitative measure of the level of agreement between the datasets from experiment and simulation[16].

1.6. It is not the intention that this CWA should provide a definitive or prescriptive methodology for the validation of a computational solid mechanics model. Instead, an objective criterion and a set of associated tools are provided that can be incorporated into a plan or strategy for verification and validation, which is appropriate to the model and its intended uses. The ASME Guide for Verification and Validation in Computational Solid Mechanics[4] provides further guidance on such plans and strategies, so that the procedures described here can be seen as complementary to the ASME guide.

[24] ADVISE, *Advanced Dynamic Validations using Integrated Simulation and Experimentation*, Project No. SCP7-GA-2008-218595, see www.dynamicvalidation.org.

[25] Burguete, R.L., Lucas, M., Patterson, E.A., Quinn, S., *Advances in Experimental Mechanics VIII*, Applied Mechanics and Materials, vol. 70, Trans Tech Publications, Durnten-Zurich, Switzerland, 2011.

2. Nomenclature

a	Distance between inner and outer loading points in the Beam Reference Material.	m
A_g	Gauge area in the Reference Material	m^2
b	Breadth of Cantilever Reference Material	m
B	Material thickness of Beam Reference Material	m
c	Distance from centre to inner loading point in Beam Reference Material	m
$d(i,j)$	Field of deviations between reference and measured values	unit of measurand
E	Young's modulus	Nm^{-2}
i,j	Pixel co-ordinates in data fields	-
$I(i, j)$	Value in image representing the measurand, e.g. a component of strain or displacement	unit of measurand
$\hat{I}(i, j)$	Reconstruction of $I(i, j)$	unit of measurand
l	Index of coefficients, i.e. component of feature vector, S	-
L	Length of cantilever in Cantilever Reference Material	m
m_E, m_T	Measurand, experimental & theoretical values	unit of measurand
n	Number of coefficients in feature vectors	-
N	Number of data points in gauge area	-
s_l	Coefficients of polynomials used for shape description	unit of measurand
S_E, S_M	Feature vector describing data from Experiment & Model, respectively	unit of measurand
$t_l(i, j)$	Tchebichef polynomials	-
T	Thickness of cantilever in Cantilever Reference Material	m
u_E, u_M	Average residual, defined by equation (3.3), for the Experiment and Model	unit of measurand
$u(d)$	Mean deviation in calibration	unit of measurand
$u(f)$	Uncertainty in measurand f	units of f

w	Displacement in z-direction	m
W	Width of gauge area in Beam Reference Material	M
x, y, z	Cartesian coordinates	m
δ	Displacement measured by single-point transducer	m
$\varepsilon(x_i, y_i)$	strain at i^{th} point (x_i,y_i)	-
$\varepsilon_{xx}, \varepsilon_{yy},$	Cartesian components of direct strain	-
ε_{xy}	Shear strain	-
η	Correction term for tensile constraint in Beam Reference Material	m
κ	Correction factor for bending constraint in Beam Reference Material	
υ	Poisson's ratio	-
λ_k, φ_k	Mode shape coefficients of the Cantilever Reference Material	-

3. Validation

3.1. Scope

3.1.1. In many engineering areas, it has been common practice to validate computational solid mechanics models using data from a single strain gauge or a set of strain gauges located in the region of maximum stress predicted by the model. This leaves results from the model not validated for the majority of the spatial domain with the possibility that, despite agreement at the location of the strain gauge, larger stress is present elsewhere in the prototype and not predicted by the model. It also exposes a risk associated with removing material from the design in areas of predicted low or zero stress in order to save weight.

Recommendation #1: *validation of computational solid mechanics models should be performed using measured full-field data maps.*

3.1.2. The advent of full-field methods of displacement and strain measurement provides the opportunity for a more comprehensive approach to be taken to the validation of computational solid mechanics models. Techniques such as digital image correlation (DIC), digital speckle pattern interferometry (DSPI) and thermoelastic stress analysis (TSA) generate data-rich fields of surface displacement or strain that might contain of the order of 10^6 data points, which is comparable to the number of individual elements or nodes in a finite element model. It is preferable to acquire this data using a calibrated instrument.

Recommendation #2: *preferably a calibrated instrument should be used to measure the data fields*.

3.1.3. However, in practice the surface of the object may need to be sub-divided for the measurement: to avoid obstructions to optical access; to achieve pseudo-planar conditions in the field of view; and to ensure sufficient spatial resolution. The latter two factors are important in reducing measurement uncertainties. While, the proportion of the surface area of the artefact over which data should be validated will depend on the purpose for which it is intended to employ the computational model.

Recommendation #3: *data should be acquired from the entire surface to which optical access can be achieved, and the surface be sub-divided as necessary to reduce measurement uncertainties.*

3.1.4. The specification of surface displacement or strain data is appropriate because of the lack of readily-available techniques for measuring displacements and strain in the interior of an engineering artefact, and because it is a natural extension of the use of strain gauges. Noting that techniques such as three-dimensional photoelasticity are only applicable to transparent materials and otherwise require transparent models, and x-ray computed tomography is limited by its cost and the size of the object that can be examined. For cases involving structural integrity, strain is the preferred measurand because structural failure is usually driven by the strain (or stress) distribution, while displacement fields could contain rigid-body components. However, displacement fields can be a more appropriate measurand in cases where modal shapes are important or shape changes influence device performance.

Recommendation #4: *the measurand(s) used for decisions about structural design or operational performance should be employed for validation purposes.*

3.1.5. It is good practice to conduct experiments specially designed for the purpose of generating data for a validation process; especially to assist in matching of data sets or regions of interest with those from the computational model. An experiment can be considered as a physical model of reality since usually it contains some level of idealisation in order to render it practical to conduct. The level of idealisation should be reduced to a minimum through the use of prototypes that come as close as possible to the manufactured artefact in terms of geometry, material and scale; and should be used with loading and boundary conditions that reproduce

those displacement or strain levels anticipated in service. There are many texts covering the topic of the design of experiments that can be consulted, e.g. [26].

3.1.6. The validation approach presented here can be divided into two parts: first, a method is described for compressing the datasets obtained from the experiment and computational model, and second, a method for correlating the data in a quantitative manner is introduced and the acceptability, or otherwise of the correlation is discussed. The complete process is shown schematically in figure 3.1. The need to validate computational models of sub-components, components, sub-elements, elements and the complete system, in a bottom-up approach, is described in ASME V&V 10-2006[4], and so is not discussed here; however, the process in figure 3.1 can be applied repeatedly to a hierarchical set of models.

3.2. Image Decomposition

3.2.1. In general, data fields obtained from experiments and computational models will be data-rich, i.e. containing data values at more than 10^4 points, will be defined in different co-ordinate systems and in arrays with different pitches, and will be orientated differently, for instance, as a result of the location of the sensor in the experiment. These factors render the direct comparison of two data fields impractical on a point-by-point basis. A practical alternative is to consider the data fields as images in which the level of the displacement or strain is represented by the grey level values of the image. Then, these images can be decomposed to feature vectors containing typically 10^2 or less shape descriptors; and, a quantitative comparison made of the feature vectors♣. Typically, shape descriptors are the coefficients of orthogonal polynomials used to describe the image; and thus, for a specified set of appropriate polynomials, contain the information required to describe uniquely the essential features of the image.

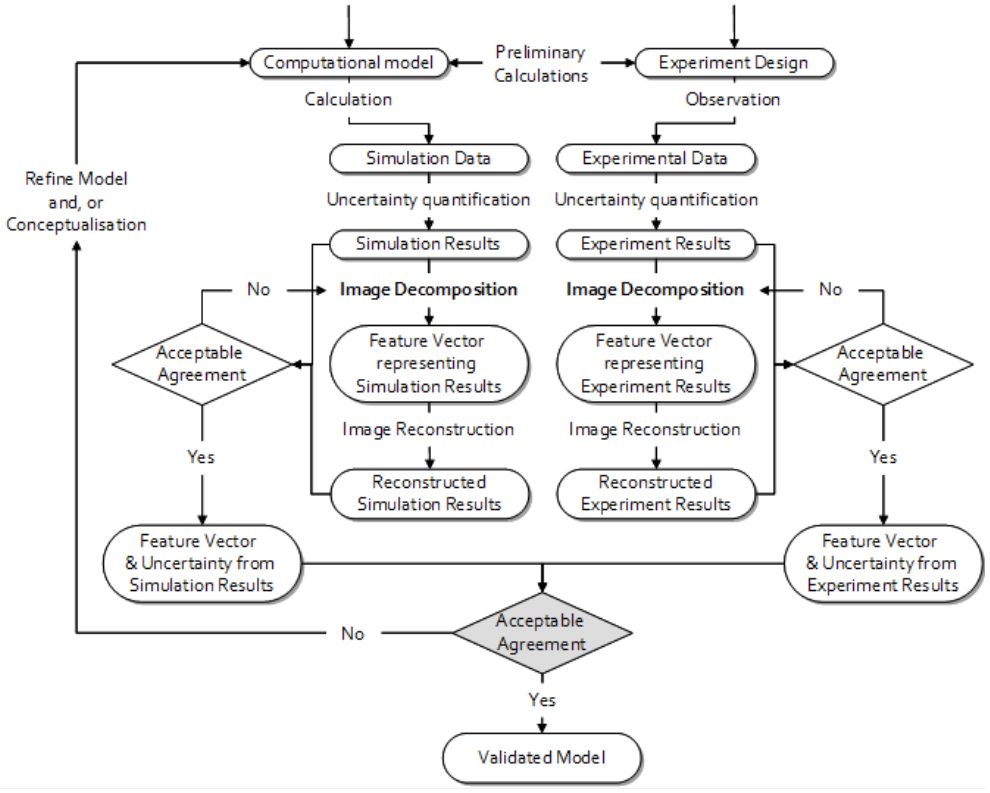

Figure 3.1 – Flow chart for the validation process using image decomposition

[26] Anthony, J., 2003, *Design of Experiments for Engineers and Scientists*, Butterworth-Heinemann, Oxford.

♣ In cases where it is preferred to use the two data fields without image decomposition, then the correlation described in section 3.3 can be employed using the corresponding points from the data fields instead of the elements of the feature vectors.

3.2.2. It is assumed here that the engineering artefact being considered is planar, or near to planar, in the each region of interest (ROI); so that the effects of three-dimensional shape and perspective on the view are negligible. These conditions could be achieved by sub-dividing the surface of the artefact as discussed in section 3.1.3.

3.2.3. The selection of an appropriate decomposition process for a displacement or strain field can generate a set of shape descriptors that are invariant to scale, rotation and translation. This invariance allows comparison of displacement or strain fields to be made using their representative shape descriptors regardless of whether the fields are in the same coordinate system, have the same scale, orientation, or sampling grid. However, the data fields from the model and experiment should have identical fields of view or regions of interest (ROI) relative to the artefact and should be based on either the deformed shape or, preferably the original shape of the component.

3.2.4. For instance, Tchebichef or Krawtchouk polynomials can be used to generate properly normalised, orthogonal shape descriptors, which are invariant to rotation, scale and translation. Tchebichef polynomials yield global shape descriptors, but it has been found that they do not provide an accurate description of strain fields when there are cut-outs or holes due to the geometry of the artefact present in the image. This issue can be handled by tailoring the moments to the individual geometry[21]; or using Krawtchouk polynomials; or by performing a fast Fourier transform on the image and then representing the magnitude component of the FFT using shape descriptors[27].

3.2.5. For example, a displacement or strain image, $I(i, j)$ can be decomposed as a series expansion of Tchebichef polynomials, $t(i, j)$

$$I(i, j) = \sum_{l=0}^{n} s_l t_l(i, j) \tag{3.1}$$

in which the coefficients s_l constitute the feature vector, S and are given by

$$s_l = \sum_{i,j}^{N} I(i, j) t_l(i, j) \tag{3.2}$$

Note that since the polynomials are dimensionless, all s_l have the same unit as the image I, i.e. displacement or strain. The identity Eq.(3.1) is exactly valid for $n=\infty$ or $n=N$ where N is the number of data points. However, typically a series expansion of order one hundred or less is sufficient.

3.2.6. It is important to consider and test the accuracy with which the feature vector represents the original data field by reconstructing the data field from the feature vector. If the reconstruction is found to be unacceptable, then steps should be taken to refine the representation until it becomes acceptable, and these steps may include employing a Fourier transform as described above, increasing the order of the expansion, selecting an alternative orthogonal shape descriptor, or tailoring of a shape descriptor.

Recommendation #5: *The goodness of fit of the reconstruction of a displacement* or *strain field to the original data field should be assessed using the average squared residual*

$$u^2 = \frac{1}{N} \sum_{i,j}^{N} \left(\hat{I}(i, j) - I(i, j) \right)^2 \tag{3.3}$$

where $\hat{I}(i, j)$ *is the reconstructed value of* $I(i, j)$*; and the average residual,* u *should be no greater than the measurement uncertainty,* u_{meas} *obtained from the instrument. In addition, no location should show a clustering of residuals greater than* $3u$*, where a cluster is defined as a group of adjacent pixels comprising 0.3% or more of* N*, the total of number of pixels in the region of interest.*

[27] Patki, AS., Patterson, EA., Decomposing strain maps using Fourier-Zernike shape descriptors, *Experimental Mechanics*, 52(8):1137-1149, 2012.

3.2.7. The process of representing the displacement or strain field by a set of shape descriptors is performed independently for the results from the computational model to be validated and those from the experiment performed for the purpose of validation, but the identical type and orders of shape descriptors must be used, resulting in two feature vectors (S_E) and (S_M). The goodness of the representation is described by the residual u, defined in equation (3.3), which at the same time constitutes the uncertainty $u(s_l)$ of the shape descriptors, s_l. When the image decomposition is made using orthonormal polynomials, this uncertainty is equal for all $l=1…n$.

3.3. Correlation of Data from Computational Model and Experiment

3.3.1. The feature vectors representing the data fields, for identical regions of interest, obtained from the computational model being validated and the experiment performed for the purpose of validation need to be compared quantitatively. The coefficients, s_l of the feature vector, S_M representing the results from the model can be plotted against those obtained from the experiment, S_E as shown in figure 3.2. If the correlation were perfect then all of the plotted data points would lie exactly on a straight line of a gradient of unity. In practice, this will not occur either due to noise in the data or because the model is a poor representation of the reality of the experiment.

Recommendation #6: *the coefficients, s_l of the feature vector representing the results from the computational model should be plotted against those obtained from the experiment.*

3.3.2. For the validation process, it is essential that a quantitative indication of the quality of experimental data is provided and the experimental uncertainty $u(S_E)$ is the natural basis for this assessment. The experimental uncertainty is estimated from the residuals u_E, using equation (3.3), but must be combined with the measurement uncertainty u_{meas}, i.e.

$$u(s_E) = \sqrt{u_{meas}^2 + u_E^2} \tag{3.4}$$

where u_{meas} can be obtained from a calibration process, such as described in section 4.

3.3.3. For an assessment of the quality of the computational model a band of acceptability can be plotted defined by the experimental uncertainty as shown in figure 3.2 and when all of the coefficients of the feature vectors fall within it then the model can be considered valid. A concordance correlation coefficient, such as proposed by Lin[28], may be used to describe the extent to which the data from the computational model represents that from the experiment.

Recommendation #7: *The computational model can be considered to be a good representation of the reality of the experiment, if all of the plotted data-points lie within a band of width $\pm 2u(s_E)$ around the ideal line, $s_M = s_E$ (see Figure 3.2), where s_M and s_E are the shape descriptors representing the displacement or strain fields from the model and experiment respectively; and $u(s_E)$ is the experimental uncertainty and should be cited when describing the validity of the model.*

3.3.4. This approach avoids the need for knowledge of the uncertainty associated with the computational model. In effect, the magnitude of the measurement uncertainty controls the level of conservatism in the validation. The definition of the acceptable experimental uncertainty is a strategic decision for each organisation since reducing it usually raises the cost of the experiment.

3.3.5. If satisfactory agreement between computational model and experimental results is not achieved according to the comparison described in recommendation #7, then the comparison process should be reviewed critically before considering refinement of the computational model. Then, according to figure 3.1, the decomposition, comparison and refinement processes should be repeated until the agreement is acceptable.

3.3.6. This validation process should be repeated for each loading case for which the fundamental mechanics of the model are changed, e.g. when moving from a linear to non-linear regime, or when the boundary conditions are changed. Similarly, the process can be applied to 'snap-

[28] Lin, L. I-K., A concordance correlation coefficient to evaluate reproducibility, *Biometrics*, 45(1):255-268, 1989

shots' acquired at instants of time from time-varying data fields, e.g. generated during cyclic or transient events

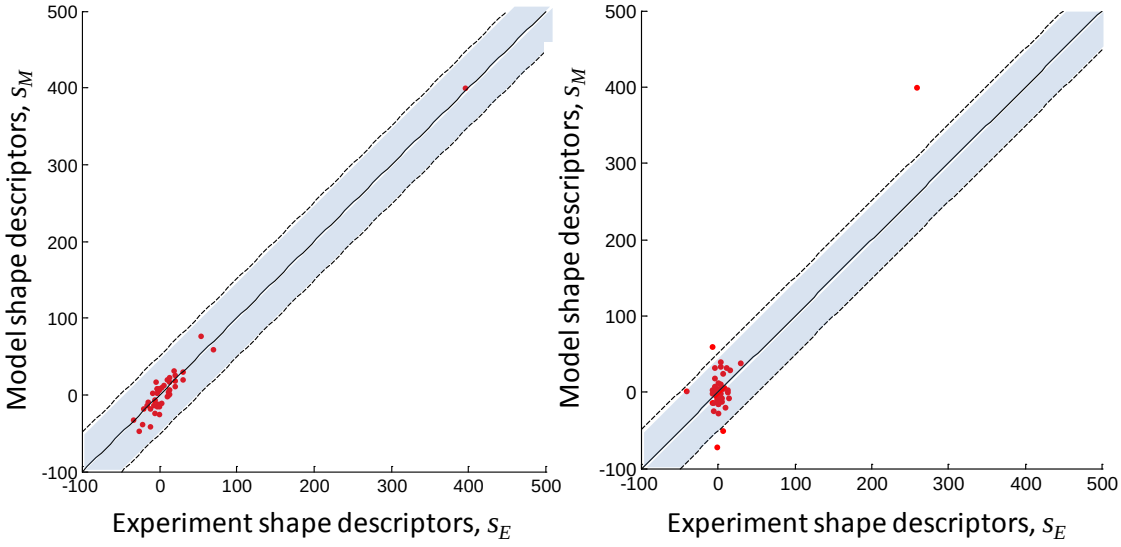

Figure 3.2 – Shape descriptors representing a displacement or strain field from a computational model, s_M plotted as a function of the shape descriptors representing the corresponding data field from the validation experiment, s_E for an acceptable (left) and unacceptable (right) validation, based on whether or not the plotted points fall within the acceptance band (shaded) defined by $s_M = s_E \pm 2u(s_E)$

4. Calibration

4.1. Scope

The purpose of this section is to describe an exemplar procedure that could be used for the calibration of optical systems for the measurement of strain or displacement fields. Calibration includes making comparisons with a known, recognized criterion or Reference Material. A continuous chain of comparisons to an international standard, each with an established measurement uncertainty provides traceability[29] thereby facilitating the use of such instruments within a regulatory environment. Traceability to international standards via length has been selected as the primary route for both strain and displacement values[30].

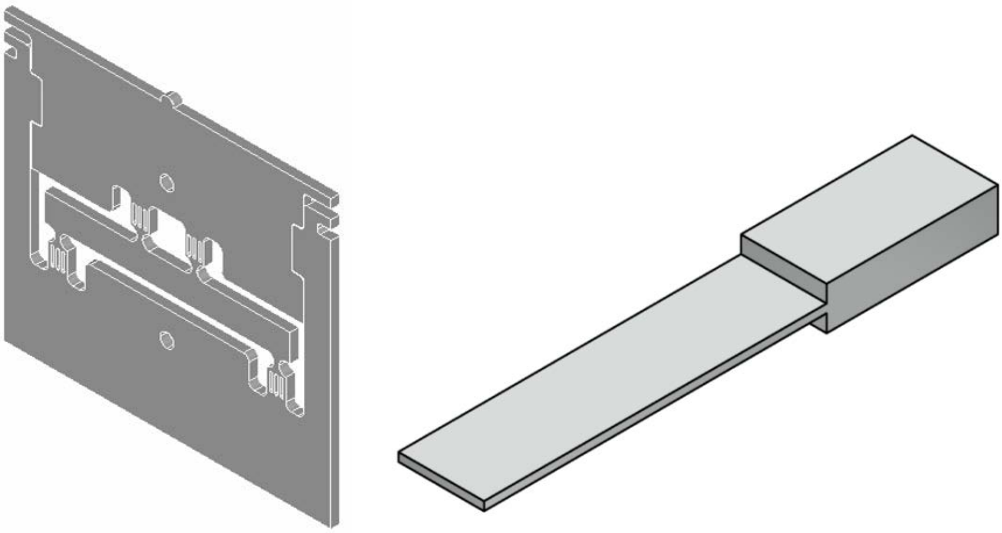

Figure 4.1 – Beam Reference Material (*EU Community Design Registration 000213467*) (left) and Cantilever RM (*right*) intended for calibration; details for the Beam RM are given in Kujawinska et al. [31].

4.2. Reference Materials

4.2.1 Reference Materials (RM) have been designed[12] to handle two classes of loading, i.e. a Beam Reference Material (Figure 4.1 left) for in-plane static or quasi-static loading and a Cantilever Reference Material (Figure 4.1 right) for out-of-plane static and cyclic loading. The Beam RM consists of a two-dimensional system for applying four-point bending to a beam of depth W. The Cantilever RM consists of a stepped bar which forms a simple cantilever of length L=40T and width b=10T where T is the thickness of the thin section (Figure 4.2).

4.2.2 The two designs proposed here are parametric, monolithic i.e. machined from a single piece of material, and can be manufactured in any homogeneous, isotropic material that is free of residual stress. The dimensions and materials should be chosen so that the spatial field of view, deformation and strain levels, and frequency are comparable to those expected to be measured with the calibrated system. However, the Reference Materials should remain in the elastic loading regime for all loading conditions so that the process is reproducible.

4.2.3 The gauge area, A_g of the Beam RM is defined as a square of dimension $W \times W$ centred on the axis of symmetry of the beam (Figure 4.2 left), with the origin of the coordinate system defined at its centre such that x is measured along the beam and y across the beam.

---

[29] ISO/IEC Guide 99: 2007, International vocabulary of metrology – Basic and general concepts and associated terms (VIM). Joint Committee for Guides in Metrology 200:2008, 3rd Ed. (BIPM, Paris 2012)

[30] Hack, E., Burguete, R.L., Patterson, E.A., Traceability of optical techniques for strain measurement, *Appl. Mechanics and Materials*, 3-4, 391-396, 2005.

[31] Kujawinska, M., Patterson, EA., Burguete, R., Hack, E., Mendels, D., Siebert, T., Whelan, M.,Calibration and assessment of full-field optical strain measurement procedures and instrumentation, in: *Speckle06*, eds. P. Slangen, C. Cerrutti, Proc. SPIE 6341 63410Q1-Q7, 2006.

4.2.4 The gauge area, A_g of the Cantilever RM is defined as the face of the cantilever surface of dimension $b \times L$ (Figure 4.2 right), with the origin of the coordinate system defined at its root and centred on the axis of symmetry of the cantilever such that x is measured along the cantilever towards the tip and y across the face of the cantilever, and z from the neutral axis through the thickness.

4.2.5 Traceability for the Beam RM is achieved by measuring the relative displacement, δ, of the top and bottom faces of the beam using an appropriate traceable device; whereas traceability for the Cantilever RM is achieved by measuring the relative deflection, δ, of the tip and the root of the cantilever using an appropriate traceable device. For the Cantilever RM used in cyclic loading, a non-contacting sensor is recommended.

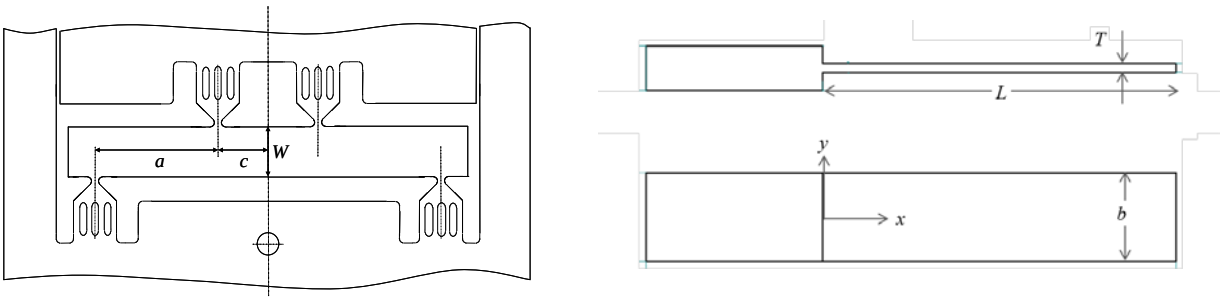

Figure 4.2 – Schematic diagrams of the Beam RM (*left*) and Cantilever RM (*right*) showing measurements whose uncertainty must be estimated.

4.3. Strain and displacement field equations

4.3.1. Beam Reference Material

The strain components inside the gauge area of the Beam RM are given by

$$\varepsilon_{xx} = \frac{\delta}{6W^2}(\kappa y + \eta), \quad \varepsilon_{yy} = -\upsilon\,\varepsilon_{xx} \quad \text{and} \quad \varepsilon_{xy} = 0 \tag{4.1}$$

where W is the depth of the beam, δ is the applied displacement and υ is Poisson's ratio

The constants κ and η are introduced to represent more accurately the strain field in the gauge section under the constraints imposed by the monolithic connection to the frame. While an ideal four-point bend has κ =1 and $\eta = 0$, the actual constants can be evaluated using a pair of strain gauges on the top and bottom surfaces of the beam.

4.3.2. Cantilever Reference Material in cyclic loading

The modal shape for resonant bending modes is given by Blevins[32]. The first bending mode is recommended for use in calibration and can be found at a frequency, f_1

$$f_1 = \frac{\lambda_1^2}{4\pi}\sqrt{\frac{E}{3\rho}}\,\frac{T}{L^2} \tag{4.2}$$

where E and ρ are Young's modulus and density of the material, respectively. The first bending mode has a shape described by

$$w_1\left(\frac{x}{L}\right) = \frac{\delta}{2}\left\{\cosh\lambda_1\frac{L-x}{L} + \cos\lambda_1\frac{L-x}{L} - \varphi_1\left(\sinh\lambda_1\frac{L-x}{L} + \sin\lambda_1\frac{L-x}{L}\right)\right\} \tag{4.3}$$

[32] Blevins, R.D., *Formulas for natural frequency and mode shape*, Krieger Pub. Co., Malabar, FA, 2001.

where w_1 is the out-of-plane displacement of the cantilever, δ is the tip amplitude, x is measured from the clamped end along the cantilever and the parameters are $\lambda_1 = 1.875$ and $\varphi_1 = 0.7340$.

The direct strain along the cantilever, ε_x is given by

$$\varepsilon_{xx}(x, y) = z \frac{d^2 w(x)}{dx^2} \tag{4.4}$$

where z is the distance from the neutral axis through the thickness of the cantilever beam, such that at the top surface $z = T/2$. The longitudinal surface strain is given by

$$\varepsilon_1(x, y) = \delta \frac{\lambda_1^2 T}{4L^2} \left\{ \cosh \lambda_1 \frac{L-x}{L} - \cos \lambda_1 \frac{L-x}{L} - \varphi_1 \left(\sinh \lambda_1 \frac{L-x}{L} - \sin \lambda_1 \frac{L-x}{L} \right) \right\} \tag{4.5}$$

4.3.3. Cantilever Reference Material in static bending

Static bending of the cantilever is introduced by a line load acting at its tip for which the out-of-plane displacement is given by Young[33]

$$w(x) = \frac{\delta}{2L^3} \left(3Lx^2 - x^3 \right) \tag{4.6}$$

and using Eq. (4.4), the direct strain along the cantilever, ε_{xx} , is given by

$$\varepsilon_{xx}(x, y) = \delta \frac{3T}{2L^2} \frac{L-x}{L} \tag{4.7}$$

4.4. Methodology for use

A flowchart that outlines the steps described below for performing a calibration is shown in figure 4.3 and should be read in conjunction with the following sections.

4.4.1. Initial testing

After manufacture the Reference Material should be measured to establish the actual dimensional values. For the Beam Reference Material beam depth, W, distance a between the loading points, and the distance c between the inner loading point and the centre of the gauge area. For the Cantilever Reference Material, the cantilever thickness T, length L, and breadth b (see figure 4.2). In both cases the uncertainty in these measurements $u(f)$, should be estimated[34] and is equal to the positive square root of the estimated variance[35].

4.4.2. Experimental set-up

4.4.2.1. Beam Reference Material

The Beam Reference Material can be loaded statically by any means that is practical and appropriate for the scale being employed. Tension loads can be applied through the two holes on the axis of symmetry, whilst compressive loads can be applied by placing the base on a platen and applying load through the half cylinder on the top to ensure alignment of the load. The loading should be displacement controlled and the displacement should be measured at the flats provided in the two top corners. The displacement, δ is taken as the average of the measurement values from each corner. Any calibrated, traceable displacement transducer which is appropriate to the scale of the Beam Reference Material may be employed.

4.4.2.2. Cantilever Reference Material in cyclic loading

[33] Young, WC., *Roark's formulas for stress & strain*, 6th ed., McGraw-Hill Book Co., New York, 1989.

[34] ISO/IEC Guide 98:1995, *Guide to the expression of uncertainty in measurements (GUM)*, Joint Committee for Guides in Metrology 100:2008 (BIPM, Paris 2008).

[35] Taylor, BN., Kuyatt, CE., *Guidelines for evaluating and expressing the uncertainty of NIST measurements results*, NIST Technical Note 1297, NIST Physics Lab, Gaithersburg, MD. 1993.

The Cantilever Reference Material should be clamped to a rigid and immovable body. Experiments have shown that the behaviour of the cantilever is independent of the clamping method and force providing there is no relative movement between the enlarged end of the Reference Material and the rigid, immovable body. The Cantilever Reference Material can be excited at a single resonant frequency, preferably the lowest, by any means that is practical and appropriate for the scale being employed and does not involve physical contact with the cantilever. It is recommended that the vibration equipment satisfies the requirements described in ISO 16063-21:2003[36]. Acoustic loading can be employed with the Cantilever Reference Material located on a suitably large rigid table. The amplitude of the displacement of the cantilever depends on the energy of the excitation and should be monitored, at the tip and the root of the cantilever, using a calibrated non-contacting single-point displacement transducer that is appropriate to the scale of the Cantilever Reference Material. The uncertainty in these measurements should be estimated.

4.4.2.3. **Cantilever Reference Material in static bending**

The Cantilever Reference Material should be clamped to a rigid and immovable body. Experiments have shown that the behaviour of the cantilever is independent of the clamping method and force providing there is no relative movement between the enlarged end of the Reference Material and the rigid, immovable body.

For static loading, the tip of the Cantilever Reference Material should be loaded in contact by any appropriate device for introducing a line force, e.g. a dead-weight suspended from a cross-bar attached to the tip. Any calibrated, traceable displacement transducer which is appropriate to the scale of the Reference Material may be employed to monitor the tip and root displacements.

4.4.3. Measurement procedure

For instrument calibration at least 80% of the field of view should be assessed. This can be performed in a single operation if the gauge area of the appropriate Reference Material occupies 80% of the field of view. When a large field of view is to be used, it may be divided into a number of equal-sized zones and a calibration performed in each zone. In the latter case, the largest uncertainty obtained should be taken as the calibration uncertainty. In every calibration the number of data points considered must be $N \geq 100$. All data points (i, j) on the gauge area must be included in the subsequent analysis.

For static loading of either Reference Material, a map of displacement or strain in the gauge area must be evaluated for an applied displacement, δ, that generates strain or displacement values larger than the maximum in the data field from the computational model it is intended to validate with data from the calibrated instrument. The RM should at all times remain in the elastic region, i.e. there should be no permanent deformation. In addition, for cyclic loading of the Cantilever RM, maps of longitudinal strain and, or out-of-plane displacement should be obtained at a frequency comparable to the frequency of excitation in the model it is intended to validate with the calibrated instrument.

4.4.4. Comparison of measured and predicted values

Employing the measurement procedure described above, values of the measurand are obtained at an array of N points within the gauge area A_g. The location of a point (i, j) within the array can be defined by the position co-ordinates (x_i, y_i) based on the coordinate definition given in section 4.2. The corresponding values of the measurand, m, i.e. the strain or displacement, in the Reference Material should be predicted using expressions (4.1), (4.3), or (4.5) to (4.7), as appropriate. Maps of the difference between the predicted values and the measured values of the measurand, m in the Reference Material, $d\,(i,\ j)$ over the gauge area, A_g should be calculated using:

$$d(i,\ j) = m_T\ (x_i, y_j) - m_E(x_i, y_j) \tag{4.8}$$

[36] ISO 16063-21 Methods for the calibration of vibration and shock transducers - part 21: vibration calibration by comparison to a reference transducer, 2003.

where m_T and m_E are the theoretical (predicted) and experimental (measured) values of the measurand.

In a perfect world there would be no differences between predicted and measured data fields so that $d(i, j)=0$. In practice, even for a high-quality measurement system the measurements will contain random uncertainty components and probably systematic uncertainty components and these could be assessed qualitatively by plotting $d(i, j)$.

In the interest of simplicity, the mean square deviation should be evaluated using:

$$u^2(d) = \frac{1}{N}\sum_{i,j}\left[d(i,j)\right]^2 \qquad (4.9)$$

When no systematic uncertainty components are present in the measurement, $u^2(d)$ comprises random components only.

4.4.5.Calculation of Reference Material uncertainty

The expressions for the combined standard uncertainty of the Reference Material, u_{RM} can be deduced using the law of propagation of uncertainty[34]. The values of the uncertainty in the dimensions, u_{dim} can be estimated from repeated measurements. The uncertainty in the displacement measurement, $u(\delta)$ will be available from the calibration of the device used to measure δ. The dimensionless u_{id} designates the uncertainty in mapping the experimental points to the theoretical position, e.g. u_{id} = 0.001 means that the points can be identified to 1/1000 of the relevant dimension of the gauge area.

The equations describing the uncertainty as a function of position and strain or displacement across the gauge area are given in Annex A. For further calculations it is recommended to use the uncertainty values averaged over the gauge area, i.e. using a single value for u_{RM} calculated using the appropriate expression in the Annex, i.e. one of equations A.8 to A.13.

Finally, the measurement uncertainty can be approximated using Eq. (4. 9) and u_{RM} such that:

$$u_{meas} = \sqrt{u^2(d) + u_{RM}^2} \qquad (4.10)$$

Stating and documenting the measurement uncertainty, u_{meas} is an essential part of a traceability procedure and hence forms an indispensable part of the validation process. The value of the measurement uncertainty, u_{meas} is used in assessing the quantitative comparison of the data fields from the computational model and the validation experiment, i.e. in equation (3.4).

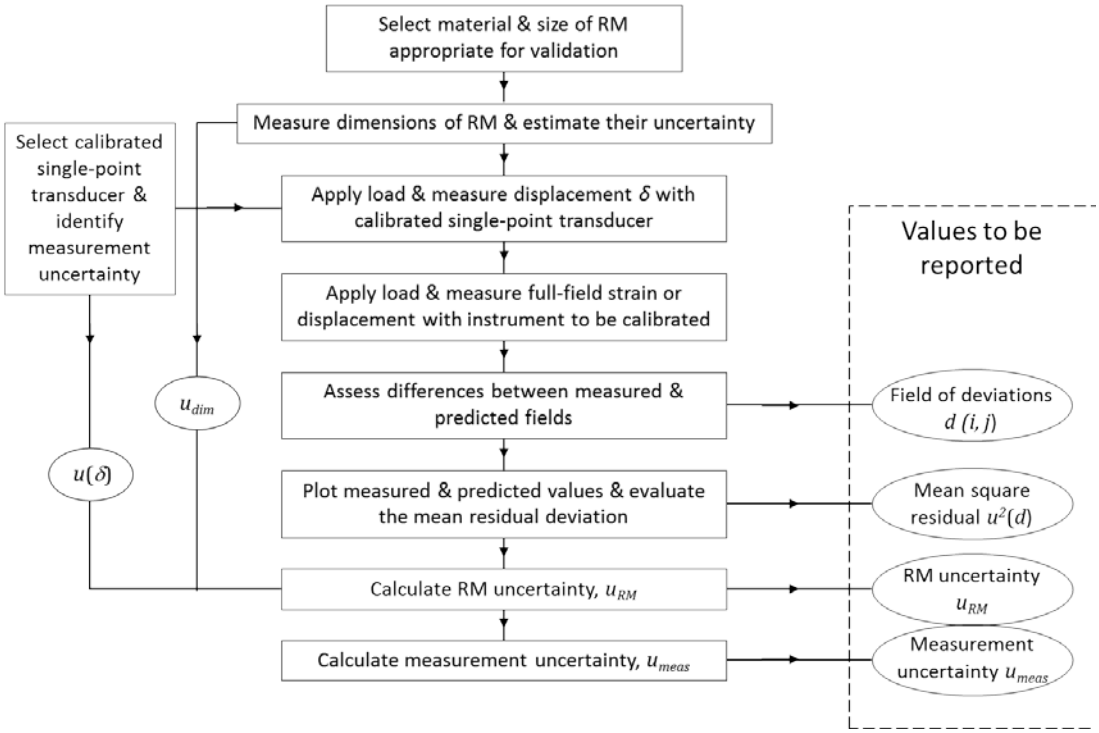

Figure 4.3 – Flow chart for performing a calibration with operations shown as rectangular boxes and quantities as ovals. Quantities that should be reported as part of a calibration are highlighted separately as outputs on the right.

Annex A

(informative)

Uncertainty estimation for the Reference Material values

The expressions for the combined standard uncertainty of the Reference Material strain values, u_{RM} can be deduced using the law of propagation of uncertainty[34] and are given below for strain and displacement measurements in the two Reference Materials.

For the Beam Reference Material the uncertainty for the longitudinal strain can be evaluated from

$$u_{RM}^2(\varepsilon_{xx}) = \varepsilon_{xx}^2\left[\frac{u^2(\delta)}{\delta^2}+\frac{u^2(\kappa)}{\kappa^2}+\frac{16u^2(W)+u^2(a)+u^2(c)}{4W^2}\right]+\left(\frac{\delta}{6W^2}\right)^2 u^2(\eta) \tag{A.1}$$

while for the strain in y-direction

$$u_{RM}^2(\varepsilon_{yy}) = \varepsilon_{yy}^2\left[\frac{u^2(\delta)}{\delta^2}+\frac{u^2(\kappa)}{\kappa^2}+\frac{16u^2(W)+u^2(a)+u^2(c)}{4W^2}+\frac{u^2(\upsilon)}{\upsilon^2}\right]+\left(\frac{\upsilon\delta}{6W^2}\right)^2 u^2(\eta) \tag{A.2}$$

For the Cantilever Reference Material in static bending from

$$u^2(\varepsilon_{xx}) = \left[\frac{u^2(\delta)}{\delta^2}+\frac{u^2(T)}{T^2}+4\frac{u^2(L)}{L^2}\right]\varepsilon_{xx}^2 \quad + \quad \left(\delta\frac{3T}{2L^2}\right)^2 u_{id}^2 \tag{A.3}$$

$$u^2(w) = \frac{u^2(\delta)}{\delta^2}w^2 \quad + \quad \delta^2\frac{9x^2}{4L^2}\left(2-\frac{x}{L}\right)^2 u_{id}^2 \tag{A.4}$$

For the Cantilever Reference Material in dynamic bending from

$$u_{RM}^2(\varepsilon_{xx}) = \left[\frac{u^2(\delta)}{\delta^2}+\frac{u^2(T)}{T^2}+4\frac{u^2(L)}{L^2}\right]\varepsilon_{xx}^2 \quad + \quad + \left[\delta\frac{T}{4}\left(\frac{\lambda_i}{L}\right)^2\lambda_k\right]^2\left\{\begin{array}{l}\sinh\lambda_k\left(\frac{L-x}{L}\right)+\sin\lambda_k\left(\frac{L-x}{L}\right)- \\ \varphi_k\left(\cosh\lambda_k\left(\frac{L-x}{L}\right)-\cos\lambda_k\left(\frac{L-x}{L}\right)\right)\end{array}\right\}^2 u_{id}^2 \tag{A.5}$$

$$u_{RM}^2(w) = \frac{u^2(\delta)}{\delta^2}w^2 \quad + \quad + \frac{\delta^2}{4}\left\{\begin{array}{l}\sinh\lambda_k\left(\frac{L-x}{L}\right)-\sin\lambda_k\left(\frac{L-x}{L}\right)- \\ \varphi_k\left(\cosh\lambda_k\left(\frac{L-x}{L}\right)+\cos\lambda_k\left(\frac{L-x}{L}\right)\right)\end{array}\right\}^2 u_{id}^2 \tag{A.6}$$

As these expressions are quite cumbersome for a daily laboratory use, the following simplifications are suggested:

- Use the value of position, strain or displacement averaged over the gauge area instead of the explicit dependence. Hence, the terms proportional to ε^2, w^2 and $f(x)^2$ are replaced by $\langle\varepsilon^2\rangle$ and $\langle w^2\rangle$, where $\langle\ \rangle$ indicate values averaged over the gauge area, A_g.
- Assume that all dimensional uncertainties are equal, because the machining tolerances as well as the measurement uncertainty using the same calliper are equal, i.e.

$$u^2(W) = u^2(a) = u^2(c) = u_{\dim}{}^2$$
$$u^2(T) = u^2(L) = u_{\dim}{}^2 \qquad \text{(A.7)}$$

- Further note that $T << L/2$ and $\kappa \approx 1$.

These assumptions, after averaging within the gauge area, lead to the following equations.

For the Beam Reference Material the variance of strain in longitudinal direction is

$$u^2_{BRM}(\mathrm{x-strain}) = \frac{\delta^2}{432\,W^2}\left[\frac{u^2(\delta)}{\delta^2} + \frac{9u_{\dim}{}^2}{2W^2} + u^2(\kappa) + 12\frac{u^2(\eta)}{W^2}\right] \qquad \text{(A.8)}$$

while for the strain in y-direction

$$u^2_{BRM}(\mathrm{y-strain}) = \frac{\upsilon^2\delta^2}{432\,W^2}\left[\frac{u^2(\delta)}{\delta^2} + \frac{9u_{\dim}{}^2}{2W^2} + \frac{u^2(\upsilon)}{\upsilon^2} + u^2(\kappa) + 12\frac{u^2(\eta)}{W^2}\right] \qquad \text{(A.9)}$$

For the Cantilever Reference Material in static bending

$$u^2_{CRM}(\mathrm{static\ strain}) = \frac{3T^2\delta^2}{4L^4}\left[\frac{u^2(\delta)}{\delta^2} + \frac{u_{\dim}{}^2}{T^2} + 3u_{id}{}^2\right] \qquad \text{(A.10)}$$

$$u^2_{CRM}(\mathrm{static\ deflection}) = \frac{u^2(\delta)}{16} + \frac{6}{5}\delta^2\,u_{id}{}^2 \qquad \text{(A.11)}$$

For the Cantilever Reference Material in first resonant bending mode

$$u^2_{CRM}(\mathrm{dyn\ strain}) \approx \frac{3T^2\delta^2}{4L^4}\left[\frac{u^2(\delta)}{\delta^2} + \frac{u_{\dim}{}^2}{T^2} + 5\,u_{id}{}^2\right] \qquad \text{(A.12)}$$

$$u^2_{CRM}(\mathrm{dyn\ deflection}) \approx \frac{u^2(\delta)}{4} + \frac{\delta^2}{3}u_{id}{}^2 \qquad \text{(A.13)}$$